Correlation between local structure and refractive index of e-beam evaporated (HfO_2–SiO_2) composite thin films

N. C. Das,[1] N. K. Sahoo,[1] D. Bhattacharyya,[1,a)] S. Thakur,[1] N. M. Kamble,[1] D. Nanda,[2] S. Hazra,[3] J. K. Bal,[3] J. F. Lee,[4] Y. L. Tai,[4] and C. A. Hsieh[4]
[1]*Applied Spectroscopy Division, Bhabha Atomic Research Centre, Mumbai 400085, India*
[2]*Coolant System Laboratory, Raja Rmanna Centre for Advanced Technology, Indore 452013, India*
[3]*Surface Physics Division, Saha Institute of Nuclear Physics, 1/AF Bidhannagar, Kolkata 700064, India*
[4]*National Synchrotron Radiation Research Center, 101 Hsin-Ann Road, Hsinchu Sience Park, Hsinchu 30076 Taiwan, Republic of China*

(Received 5 March 2010; accepted 17 June 2010; published online 29 July 2010)

In the present work we have reported the results of investigations on local structures of e-beam evaporated (HfO_2–SiO_2) composite thin films by synchrotron based extended x-ray absorption fine structure measurements. It has been observed that for the composite film with 10% SiO_2 content, both Hf–O and Hf–Hf bond lengths are less than their values in pure HfO_2 film. However the bond lengths subsequently increase to higher values as the SiO_2 content in the composite films is increased further. It has also been observed that at the same composition of 10% SiO_2 content, the films have smallest grain sizes (as obtained from atomic force microscopy measurements) and highest refractive index (as obtained from spectroscopic ellipsometry (SE) measurements) which suggests that the e-beam evaporated HfO_2–SiO_2 composite films with 10% SiO_2 content leads to the most compact amorphous thin film structure. © *2010 American Institute of Physics*. [doi:10.1063/1.3465328]

I. INTRODUCTION

Hafnium oxide (HfO_2) has extensively been studied as a promising high-K dielectric[1,2] to replace conventional silicon oxide (SiO_2) gate dielectric in the complementary metal-oxide semiconductor technology due to its high melting point, relatively high refractive index and its superior thermal and chemical stability in contact with silicon. It is well established that amorphousness is highly desirable in high-K gate oxide materials for their application in metal-oxide semiconductor devices since the absence of grain boundaries in amorphous materials prevents the leakage current.[3] Addition of SiO_2 in HfO_2 has shown to increase its crystallization temperature to higher value, enabling appearance of amorphous phases upto a higher temperature. Afify *et al.*[4,5] have reported an enhancement of crystallization temperature upto 1060 °C for HfO_2–SiO_2 powder prepared by sol-gel technique, while Neumayer and Cartier[6] have reported a crystalliastion temperature of 1000 °C for spin coated HfO_2–SiO_2 composite films. Increase in crystallization temperature has also been reported by Morais *et al.*[7] for reactively sputtered HfSiO films deposited from a HfSi target. Since HSO (HfO_2–SiO_2 binary oxide mixture) is found to be thermodynamically stable in contact with Si, it is being considered as a potential replacement for SiO_2 as gate dielectric material in CMOS transistor.[8]

HfO_2 has also been exploited as a high refractive index material for fabrication of multilayer dielectric coatings.[9] Use of HfO_2–SiO_2 composite film in lieu of pure HfO_2 has been explored[10,11] for tuning the band gap and refractive index of the high index layer which ultimately leads to the development of multilayer optical coatings with relatively smaller number of layers and also helps in extending the range of its application to deep UV. Retention of the amorphousness of the composite film is an important criterion also for its application in optical multilayer coatings since amorphous structure with small grain size leads to high density and high refractive index in thin films.[10] Thus HfO_2–SiO_2 composite film together with its amorphous microstructure is useful in fabrication of rugate filters and other special multilayers, that require intermediate refractive index, not available from standard materials.[12]

Though several authors have so far reported preparation of HfO_2–SiO_2 composite films and its characterizations by different techniques,[4,6,8] a systematic atomic scale local structure investigations on the composite films over a large range of SiO_2 content still remains to be explored. In the present study, the local structures of the reactive e-beam evaporated pure HfO_2 and composite HfO_2–SiO_2 films have been investigated by synchrotron based extended x-ray absorption fine structure (EXAFS) technique which is an element specific tool and can be applied to both crystalline and amorphous structures. The bond length variations observed in the (HfO_2–SiO_2) composite films as a function of composition have been correlated with their refractive index variation as reported by us earlier.[11]

II. EXPERIMENTAL SECTION

The thin film samples were deposited in a fully automatic box coating unit "VERA-902" (Vacuum Technique, Dresden) adopting reactive electron beam evaporation technique.[13] This coating system is equipped with three 8 kW electron beam guns which are interfaced with the pro-

a)Electronic mail: dibyendu@barc.gov.in.

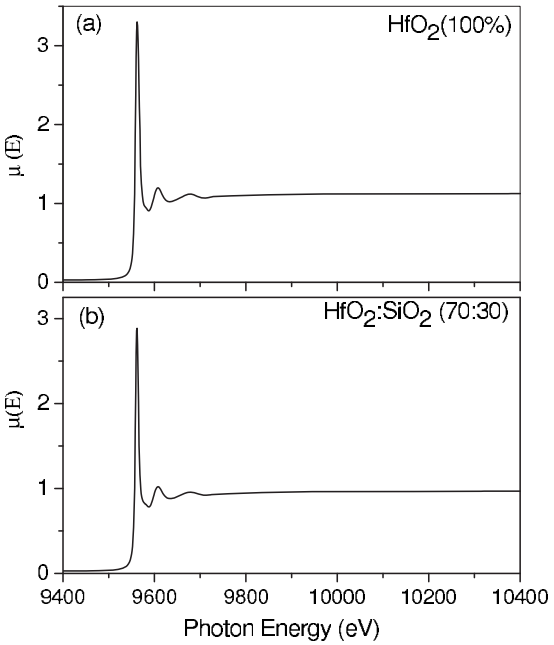

FIG. 1. μ vs E spectra of (a) pure HfO_2 and (b) a representative composite thin films with (HfO_2:SiO_2) ratio of (70:30).

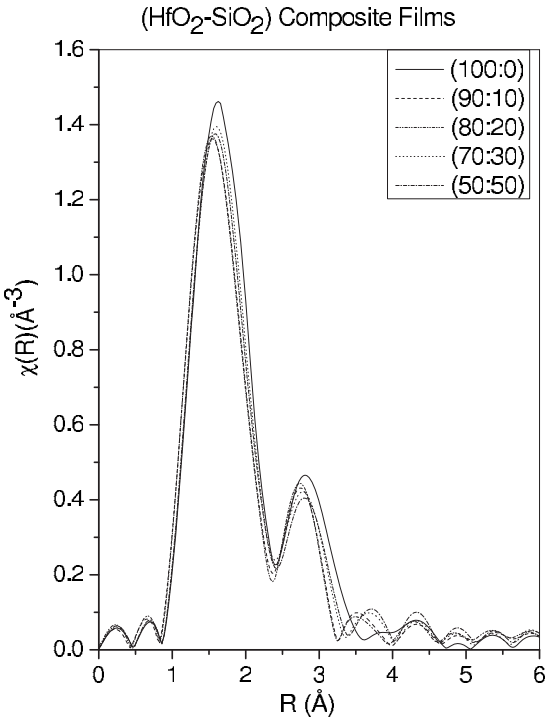

FIG. 2. $\chi(R)$ vs R spectra of a pure HfO_2 and composite thin films with (HfO_2:SiO_2) ratio of (90:10), (80:20), (70:30), and (50:50).

cess controllers along with Inficon's XTC/2 quartz crystal monitors and Leybold's OMS-2000 optical thickness monitors. For the preparation of the present set of HfO_2-SiO_2 composite films by codeposition, 99.9% pure HfO_2 and SiO_2 were evaporated simultaneously from two different e-beam sources. During the deposition process the substrate (quartz) temperature was maintained at 350 °C and high purity O_2 is bleeded into the system to compensate for the dissociation of the oxide evaporants. The O_2 flow is controlled by a MKS mass flow controller so that pressure inside the chamber remained constant at $\sim 1\times 10^{-4}$ mbar during deposition. The evaporation rates from individual sources were detected and monitored dynamically by the crystal monitors. Using the above process control, HfO_2-SiO_2 composite films with different HfO_2 to SiO_2 ratio had been prepared.

EXAFS experiments on the above mentioned thin film samples were carried out at the BL17C1 beamline on the Twaiwan Light Source (1.5 Gev, 300 mA) at the National Synchrotron Radiation Research Center, Hsinchu, Taiwan. The beamline uses a Si(111) double crystal monochromator (DCM) and the measurements have been carried out in the fluorescence mode at the L_3 absorption-edge of hafnium with Fe foil as a reference material for on-line calibration of the monochromator.

Grazing incidence x-ray diffraction (GIXRD) measurements on these films have been carried out using Cu K_α radiation in a versatile diffractometer (Model D8, Discover, Bruker AXS). Since the measurements have been carried out on thin film samples the data were recorded by keeping the incident angle fixed at a grazing angle in order to keep the probing region of the sample near its surface.

III. RESULTS AND DISCUSSION

Figure 1 shows the experimental EXAFS (μ versus E) spectra of the pure HfO_2 and a representative composite film having HfO_2:SiO_2 ratio of (70:30) measured at the Hf L_3 edge. Since the oscillations in the absorption spectra are important, the experimentally obtained μ versus E data are first converted to $\chi(E)$ versus E, where $\chi(E)$ is defined as follows:[14]

$$\chi(E) = \frac{\mu(E) - \mu_0(E)}{\Delta\mu_0(E_0)}, \tag{1}$$

where, E_0 is the absorption edge, $\mu_0(E)$ is the bare atom background, and $\Delta\mu_0(E_0)$ is the step in the $\mu(E)$ value at the absorption edge. The energy scale is also converted to the wave number scale k, given by:

$$k = \sqrt{\frac{2m(E-E_0)}{\hbar^2}}, \tag{2}$$

$\chi(k)$ is weighted by k^2 to amplify the oscillations at high k and finally the $\chi(k)k^2$ versus k spectra is Fourier transformed to generate the $\chi(R)$ versus R spectra in terms of real distances from the center of the absorbing atom.

Figure 2 shows the $\chi(R)$ versus R spectra of pure HfO_2 and composite thin films having varying (HfO_2:SiO_2) ratios of (90:10), (80:20), (70:30), and (50:50) respectively. Qualitative comparison of the above spectra with that presented by Afify *et al.*[4,5] for amorphous and crystalline HfO_2-SiO_2 samples shows that the present set of spectra resembles more to that of the amorphous phase. However, it may also be seen from Fig. 2 that the intensities of the first shell and the second shell peaks are less in the composite films compared to that in pure HfO_2 film manifesting enhancement of amorphousness in the composite films compared to the polycrystalline nature of pure HfO_2 film as reported by other workers also1.[5,15,16] It may also be seen from Fig. 2 that the first shell

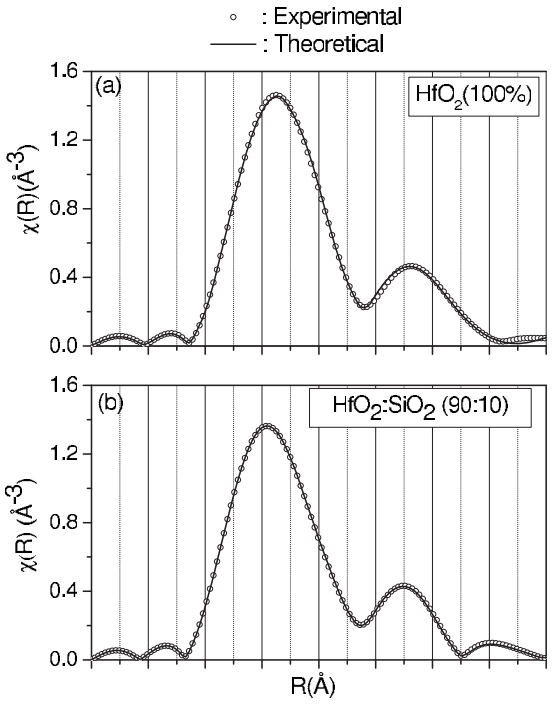

FIG. 3. Experimental $\chi(R)$ vs R spectra with best-fit theoretical plots for (a) pure HfO_2 and (b) a representative composite thin films with (HfO_2:SiO_2) ratio of (90:10).

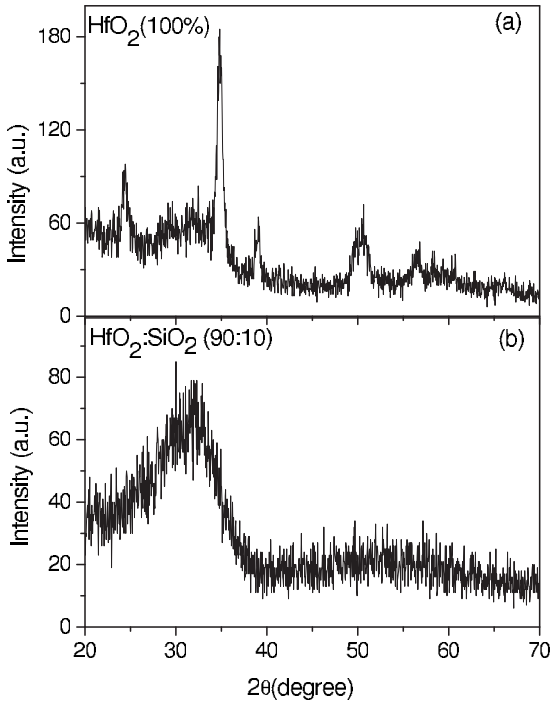

FIG. 4. XRD pattern of (a) pure HfO_2 and (b) a representative composite thin films with (HfO_2:SiO_2) ratio of (90:10).

peak intensity is lowest corresponding to the film having silica concentration of 10% indicating that the film is highly amorphous. The above observation is consistent with our earlier detail morphological studies on these samples by atomic force microscopy (AFM) where it was observed that with the incorporation of 10% SiO_2 in HfO_2 films, there is an improvement of morphological parameters of the films compared to pure HfO_2 film with a decrease in power spectral density function, improvement in height-height correlation function, decrease in surface roughness and evolution of a perfect Gaussian grain structure dsitribution.[11]

The experimental $\chi(R)$ versus R spectra for the pure HfO_2 film and the representative composite film with HfO_2:SiO_2 ratio of (90:10) have been shown in Figs. 3(a) and 3(b), respectively. It can be seen from the above figures qualitatively that, apart from the decrease in peak heights, there is a clear shift in both the first and second shell peaks of the composite film toward lower R values depicting decrease in the (Hf–O) and (Hf–Hf) bond lengths due to increase in amorphousness of the sample. In order to extract quantitative information on the bond distance (R) and coordination number of the neighboring atoms (N) around the Hf atom, the experimental $\chi(R)$ versus R spectra have been fitted with theoretical spectra. It should be mentioned here that a set of EXAFS data analysis program available within the IFEFFIT package was used for the above analysis.[17] This includes data reduction and Fourier transform to derive the $\chi(R)$ versus R spectra from the absorption spectra, generation of the theoretical EXAFS spectra starting from an assumed crystallographic structure and finally fitting of the experimental data with the theoretical spectra using the FEFF 6.0 code. The bond distances, co-ordination numbers (including scattering amplitudes) and Debye–Waller factors (σ^2), which give the mean-square fluctuations in the distances, have been used as fitting parameters. The best fit theoretical spectra for the pure HfO_2 film and the HfO_2–SiO_2 composite film have also been shown in Figs. 3(a) and 3(b) along with the experimental spectra. As extracted from the fitting of $\chi(R)$ versus R spectrum, the peak with highest intensity corresponds to the (Hf–O) bond whereas the remaining two peaks correspond to two separate (Hf–Hf) bonds.

The crystalline structure of the pure HfO_2 film has been confirmed by the GIXRD measurements, the spectrum (intensity versus 2θ) being shown in Fig. 4(a). The peaks in the spectrum have been compared with the standard reference data[18] of HfO_2 for different possible crystalline phases, viz., monoclinic, tetragonal and orthorhombic,[6,16,19,20] however, the XRD spectrum of the HfO_2 film, though having few distinctive peaks, does not correspond preferentially to any of the above structure and thus indicates mixed-phase or random polycrystalline nature of the sample. GIXRD spectra of the HfO_2–SiO_2 composite films, on the other hand, show amorphous-like broad features. The XRD spectrum of the composite film with HfO_2:SiO_2 ratio of 90:10 being shown in Fig. 4(b) where all the sharp XRD features are found to disappear confirming a homogenous amorphous structure. Since the local structures for polycrystalline and amorphous phases are generally similar, the theoretical EXAFS spectra of pure HfO_2 and composite HfO_2–SiO_2 films have been simulated assuming amorphous nature of the samples.

The local structural parameters for the first two coordination shells around the Hf-atom, as extracted from the fitting of the experimental Fourier transform (FT) spectra of the different samples with their respective theoretical spectra, have been summarized in Table I along with the expected uncertainties. It may be seen that both the Hf–O and Hf–Hf

TABLE I. Structural parameters bond length (R) and coordination number (N) corresponding to first (Hf–O) and second (Hf–Hf) coordination shells around hafnium atom in thin film samples of pure HfO_2 and (HfO_2:SiO_2) composite as obtained from EXAFS data analysis.

Sample		(HfO_2–SiO_2) (100%–0%)	(HfO_2–SiO_2) (90%–10%)	(HfO_2–SiO_2) (80%–20%)	(HfO_2–SiO_2) (70%–30%)	(HfO_2–SiO_2) (50%–50%)
First coordination shell (Hf–O)	N (atoms)	7 ± 0.2	7 ± 0.3	7 ± 0.3	6 ± 0.2	6 ± 0.2
	R(Å)	2.189 ± 0.005	2.146 ± 0.005	2.172 ± 0.006	2.181 ± 0.005	2.190 ± 0.006
	σ^2(Å^2)	0.0317 ± 0.001	0.0052 ± 0.001	0.0039 ± 0.002	0.0113 ± 0.002	0.0252 ± 0.002
Second coordination shell (Hf–Hf)	N (atoms)	7 ± 0.3	7 ± 0.3	7 ± 0.2	6 ± 0.2	5 ± 0.3
	R(Å)	3.448 ± 0.005	3.405 ± 0.006	3.431 ± 0.005	3.441 ± 0.005	3.439 ± 0.006
	σ^2(Å^2)	0.0317 ± 0.001	0.0052 ± 0.002	0.0039 ± 0.001	0.0113 ± 0.001	0.0252 ± 0.002

bond lengths (R) and coordination numbers (N) change with the variation in silica compositions in the samples. It can be seen that the bond lengths are less for the composite films with 10% SiO_2 content compared to pure HfO_2 film. However, the bond lengths increase with the increase in SiO_2 content in the composite films beyond 10%. The σ^2 values (which gives the average fluctuation in the bond lengths) is also found to be minimum for the film with SiO_2 content of 10%. The results also agree well with the trend reported by Affify *et al.*[4,5] who have also found that for sol-gel deposited amorphous HfO_2–SiO_2 films, Hf–O and Hf–Hf bond lengths are less compared to pure HfO_2 compound and the bond lengths increase as the crystallinity of the samples improves with annealing. The above facts along with the AFM results, reported earlier,[11] suggest that HfO_2–SiO_2 composite films described here with 10% SiO_2 content leads to the most compact amorphous structure.

To investigate the dielectric response of the above films on their local atomic distribution, efforts have been given to correlate the variation in bond lengths with the change in refractive index of the composite (HfO_2–SiO_2) films. Figure 5 shows the variation in refractive index (@550 nm), along with the probable uncertainties in its value, with the silica percentage in the composite (HfO_2–SiO_2) films based on our ellipsometric measurements as reported earlier.[11] It may be seen that the refractive index for the composite film with 10% SiO_2 content is higher than that of pure HfO_2, though it subsequently decreases continuously with the increase in silica percentage beyond 10% in the films. The (Hf–O) and (Hf–Hf) bond lengths for the composite (HfO_2–SiO_2) films obtained from the EXAFS measurements are also shown in Fig. 5 along with the probable uncertainties in their values. The above figure clearly reveals a strong correlation between the refractive index and the local structure of the composite HfO_2–SiO_2 films. The refractive index of the films increases as the bond lengths decrease with the maximum value of the refractive index being obtained for the sample with the 10% silica content which is also having minimum values of the (Hf–O) and (Hf–Hf) bond lengths. Beyond 10% of silica composition in the composite films, refractive index decreases as the bond lengths increase. It may be mentioned that the variation in refractive index and dielectric constant with the variation in (Si–Si) bond length has also been reported by Yeh and Chen[21] for SiO_2 thin films annealed at different temperatures.

IV. SUMMARY AND CONCLUSIONS

In summary, local structures of e-beam evaporated pure HfO_2 and composite (HfO_2–SiO_2) thin films have been investigated by EXAFS analysis. Variation in bond lengths around hafnium atom with the change in silica percentage in the composite thin films of (HfO_2–SiO_2) as obtained by the EXAFS studies is correlated with the change in refractive index of the films. It has been confirmed that as the silica percentage increases in the composite film, both Hf–O and Hf–Hf bond lengths decrease initially to attain minimum values and subsequently increase to higher values resulting in the decrease in refractive index. The lowest values of the bond lengths occur when the refractive index of the composite thin film is maximum corresponding to 10% silica content in the film which is also having highly amorphous microstructure with smoother morphological properties.

ACKNOWLEDGMENTS

The present work was carried out through the generous financial support from DAE-BRNS, Mumbai, India.

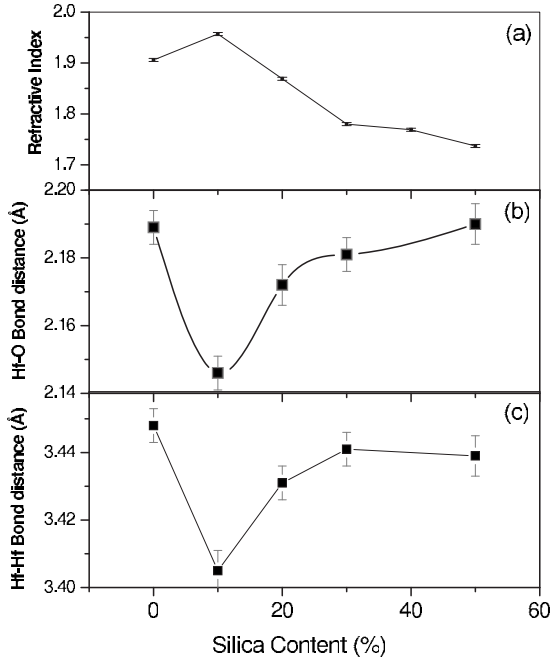

FIG. 5. (a) Variation in refractive index with the silica percentage in the composite (HfO_2:SiO_2) thin film. (b) Variation in Hf–O bond length with the silica percentage in the composite (HfO_2:SiO_2) thin film. (c) Variation in Hf–Hf bond length with the silica percentage in the composite (HfO_2:SiO_2) thin film.

[1]G. D. Wilk, R. M. Wallace, and J. M. Anthony, J. Appl. Phys. **89**, 5243 (2001).
[2]J. Robertson, Rep. Prog. Phys. **69**, 327 (2006).
[3]D.-Y. Cho, T. J. Park, K. D. Na, J. H. Kim, and C. S. Hwang, Phys. Rev. B **78**, 132102 (2008).
[4]N. D. Afify, G. Dalba, U. M. K. Koppolu, C. Armellini, Y. Jestin, and F. Rocca, Mater. Sci. Semicond. Process. **9**, 1043 (2006).
[5]N. D. Afify, G. Dalba, and F. Rocca, J. Phys. D: Appl. Phys. **42**, 115416 (2009).
[6]D. A. Neumayer and E. Cartier, J. Appl. Phys. **90**, 1801 (2001).
[7]J. Morais, L. Miotti, K. P. Bastos, S. R. Teixeira, I. J. R. Baumvol, A. L. P. Rotondaro, J. J. Chambers, M. R. Visokay, L. Colombo, and M. C. Martins Alves, Appl. Phys. Lett. **86**, 212906 (2005).
[8]L. Armelao, D. Bleiner, V. Di Noto, S. Gross, C. Sada, U. Schubert, E. Tondello, H. Vonmont, and A. Zattin, Appl. Surf. Sci. **249**, 277 (2005).
[9]M. Grilli, F. Menchini, A. Piegari, D. Alderighi, G. Toci, and M. Vannini, Thin Solid Films **517**, 1731 (2009).
[10]S. M. Edlou, A. Smajkiewicz, and G. A. Al-Jumaily, Appl. Opt. **32**, 5601 (1993).
[11]R. B. Tokas, N. K. Sahoo, S. Thakur, and N. M. Kamble, Curr. Appl. Phys. **8**, 589 (2008).
[12]Y. Tsou and F. C. Ho, Appl. Opt. **35**, 5091 (1996).
[13]N. K. Sahoo, S. Thakur, D. Bhattacharyya, and N. C. Das, Report No. BARC/1999/E/039, 1999, pp. 1–33.
[14]*X-Ray Absorption: Principles, Applications, Techniques of EXAFS, SEXAFS and XANES*, edited by D. C. Konigsberger and R. Prince (Wiley, New York, 1988).
[15]M. A. Sahiner, J. C. Woicik, P. Gao, P. McKeown, M. C. Croft, M. Gartman, and B. Benapfla, Thin Solid Films **515**, 6548 (2007).
[16]V. Gritsenko, D. Gritsenko, S. Shaimeev, V. Aliev, K. Nasyrov, S. Erenburg, V. Tapilin, H. Wong, M. C. Poon, J. H. Lee, J.-W. Lee, and C. W. Kim, Microelectron. Eng. **81**, 524 (2005).
[17]M. Newville, B. Ravel, D. Haskel, J. J. Rehr, E. A. Stern, and Y. Yacoby, Physica B **208–209**, 154 (1995).
[18]PCPDFWIN, PDF No. 89-1813; http://www.icdd.com; International Centre for Diffraction Data, PA.
[19]P. S. Lysaght, J. C. Woicik, M. A. Sahiner, B.-H. Lee, and R. Jammy, Appl. Phys. Lett. **91**, 122910 (2007).
[20]R. C. Smith, T. Ma, N. Hoilien, L. Y. Tsung, M. J. Bevan, L. Colombo, J. Roberts, S. A. Campbell, and W. L. Gladfelter, Adv. Mater. Opt. Electron. **10**, 105 (2000).
[21]C. F. Yeh and T. J. Chen, Appl. Phys. Lett. **70**, 1611 (1997).